Medicine®

DIAGNOSTIC ACCURACY STUDY

OPEN

A Pilot Comparison of ^{18}F-fluorocholine PET/CT, Ultrasonography and ^{123}I/^{99m}Tc-sestaMIBI Dual-Phase Dual-Isotope Scintigraphy in the Preoperative Localization of Hyperfunctioning Parathyroid Glands in Primary or Secondary Hyperparathyroidism

Influence of Thyroid Anomalies

Laure Michaud, MD, Sona Balogova, MD, PhD, Alice Burgess, MD, Jessica Ohnona, MD, Virginie Huchet, MD, Khaldoun Kerrou, MD, Marine Lefèvre, MD, Marc Tassart, MD, Françoise Montravers, MD, PhD, Sophie Périé, MD, PhD, and Jean-Noël Talbot, MD, PhD

Abstract: We compared ^{18}F-fluorocholine hybrid positron emission tomography/X-ray computed tomography (FCH-PET/CT) with ultrasonography (US) and scintigraphy in patients with hyperparathyroidism and discordant, or equivocal results of US and ^{123}I/^{99m}Tc-sesta-methoxyisobutylisonitrile (sestaMIBI) dual-phase parathyroid scintigraphy. FCH-PET/CT was performed in 17 patients with primary (n = 11) lithium induced (n = 1) or secondary hyperparathyroidism (1 dialyzed, 4 renal-transplanted).

The reference standard was based on results of surgical exploration and histopathological examination. The results of imaging modalities were evaluated, on site and by masked reading, on per-patient and per-lesion bases.

In a first approach, equivocal images/foci were considered as negative. On a per-patient level, the sensitivity was for US 38%, for scintigraphy 69% by open and 94% by masked reading, and for FCH-PET/CT 88% by open and 94% by masked reading. On a per-lesion level, sensitivity was for US 42%, for scintigraphy 58% by open and 83% by masked reading, and for FCH-PET/CT 88% by open and 96% by masked reading. One ectopic adenoma was missed by the 3 imaging modalities. Considering equivocal images/foci as positive increased the accuracy of the open reading of scintigraphy or of FCH-PET/CT, but not of US. FCH-PET/CT was significantly superior to US in all approaches, whereas it was more sensitive than scintigraphy only for open reading considering equivocal images/foci as negative ($P = 0.04$). FCH uptake was more intense in adenomas than in hyperplastic parathyroid glands. Thyroid lesions were suspected in 9 patients. They may induce false-positive results as in one case of oncocytic thyroid adenoma, or false-negative results as in one case of intrathyroidal parathyroid adenoma. Thyroid cancer (4 cases) can be visualized with FCH as with ^{99m}Tc-sestaMIBI, but the intensity of uptake was moderate, similar to that of parathyroid hyperplasia.

This pilot study confirmed that FCH-PET/CT is an adequate imaging tool in patients with primary or secondary hyperparathyroidism, since both adenomas and hyperplastic parathyroid glands can be detected. The sensitivity of FCH-PET/CT was better than that of US and was not inferior to that of dual-phase dual-isotope ^{123}I/^{99m}Tc-scintigraphy. Further studies should evaluate whether FCH could replace ^{99m}Tc-sestaMIBI as the functional agent for parathyroid imaging, but US would still be useful to identify thyroid lesions.

(*Medicine* 94(41):e1701)

Abbreviations: FCH = ^{18}F-fluorocholine, FDG = ^{18}F-fluorodeoxyglucose, FDOPA = ^{18}F-fluorodihydroxyphenylalanine, FN = false negative, PET/CT = hybrid positron emission tomography/X-ray computed tomography, PTH = parathyroid hormone, sestaMIBI = sesta-methoxyisobutylisonitrile, SNM = Society of Nuclear Medicine, SPECT/CT = hybrid single-photon emission computed tomography/X-ray computed tomography, SUVmax = maximal standardized uptake value, TN = true negative, TP = true positive, US = ultrasonography.

INTRODUCTION

Recently published cases have described incidentally discovered parathyroid adenomas with ^{11}C-choline[1] or ^{18}F-fluorocholine (FCH)[2–4] hybrid positron emission tomography/X-ray computed tomography (PET/CT) imaging performed for the evaluation of prostate cancers. FCH, and also ^{18}F-fluorodeoxyglucose (FDG), can be produced industrially and distributed to several PET centers; its logistics is easier than that of ^{11}C-choline. FCH-PET/CT is a validated diagnostic tool in the management of patients with prostate cancer or hepatocellular carcinoma,[5–7] but it may be positive in other cancers, in nonmalignant tumors, or in inflammatory lesions.[3,8,9] In 2014, preliminary results have confirmed that PET/CT with

Editor: Gaurav Malhotra.
Received: February 23, 2015; revised: August 5, 2015; accepted: September 7, 2015.
From the Department of Nuclear Medicine, Hôpital Tenon, Assistance Publique Hôpitaux de Paris, Paris, France (LM, SB, JO, VH, KK, FM, J-NT); Department of Nuclear Medicine, Comenius University & St. Elisabeth Oncology Institute, Bratislava, Slovakia (SB); Department of Otolaryngology Head and Neck Surgery, Hôpital Tenon, Assistance Publique Hôpitaux de Paris (AB, SP); Faculté de Médecine Pierre et Marie Curie (JO, FM, SP, J-NT); Department of Pathology, Hôpital Tenon, Assistance Publique Hôpitaux de Paris (ML); and Department of Radiology, Hôpital Tenon, Assistance Publique Hôpitaux de Paris, Paris, France (MT).
Correspondence: Professor Jean-Noël Talbot, Médecine Nucléaire Hôpital Tenon, 4, rue de la Chine, F75020 Paris, France (e-mail: jean-noel.talbot@aphp.fr).
The authors have no funding and conflicts of interest to disclose.

ISSN: 0025-7974
DOI: 10.1097/MD.0000000000001701

^{11}C-choline[10] or FCH,[11,12] performed deliberately in patients with primary hyperparathyroidism and no prostate cancer, is able to localize hyperfunctioning parathyroid glands. In case of primary hyperparathyroidism, the diagnostic performance of FCH-PET/CT was at least as good as that of scintigraphy with ^{99m}Tc-sesta-methoxyisobutylisonitrile (sestaMIBI)[11] and hyperfunctioning parathyroid glands can be detected while scintigraphy with ^{99m}Tc-sestaMIBI was negative or equivocal.[12] Our own preliminary study, published in 2014,[13] also showed that FCH-PET/CT is able to localize not only the parathyroid adenomas in case of primary hyperparathyroidism, but also the hyperplastic glands in case of hyperparathyroidism secondary to renal failure.

In patients with secondary hyperparathyroidism, and also with primary hyperparathyroidism, an accurate localization of all hyperfunctioning parathyroid glands is critical before surgery. In patients with primary hyperparathyroidism, a minimally invasive surgery focused on the hyperfunctioning parathyroid gland is commonly performed. In contrast, secondary hyperparathyroidism, in a dialyzed patient or persisting after renal transplantation, requires the surgeon to localize preoperatively all parathyroid glands, to remove most of the hyperplastic parathyroid tissue. Preoperative ultrasonography (US) and scintigraphy using ^{99m}Tc-sestaMIBI are documented imaging modalities in both situations,[14–17] as they bring complementary anatomical and functional information. In cases of negative or doubtful results of imaging or of discrepant results between scintigraphy and US, it is important to rely on another imaging modality. According to the preliminary results, FCH-PET/CT could be this modality,[11–13] but a comparison of diagnostic performance has not been performed with the reference functional modality, ^{99m}Tc-sestaMIBI scintigraphy, in series including patients with secondary hyperparathyroidism and/or with anomalies of the thyroid gland. In secondary hyperparathyroidism, small-sized hyperplastic parathyroid glands are predominant, with a reduced sensitivity of US and ^{99m}Tc-sestaMIBI scintigraphy, when compared to parathyroid adenomas.[16] In case of thyroid anomalies, both false-positive and false-negative results may occur due to confusing thyroid nodules and abnormal parathyroid glands on US and on ^{99m}Tc-sestaMIBI scintigraphy as thyroid lesions may be sestaMIBI avid.[18–20] Thyroid anomalies interfere less in case of solitary parathyroid adenoma than in case of multiglandular parathyroid disease.[21] The present study was designed to compare the diagnostic performance of FCH-PET/CT, ^{99m}Tc-sestaMIBI scintigraphy and US in a pilot series including patients with secondary hyperparathyroidism and/or anomalies of the thyroid gland, postsurgical histology being the reference standard. FCH maximal standardized uptake value (SUVmax) of the suspected parathyroid glands and the ratio of SUVmax between the parathyroid glands and the neighboring thyroid tissue were also determined.

MATERIALS AND METHODS

Patients

^{18}F-fluorocholine hybrid positron emission tomography/X-ray computed tomography was proposed to patients with hyperparathyroidism scheduled for surgery, when the surgical procedure to cure hyperparathyroidism was uncertain due to discrepancies between US and ^{99m}Tc-sestaMIBI scintigraphy, or due to equivocal images on one of those imaging modalities. Patients were informed that FCH was a registered diagnostic agent in France.[7] The use of FCH-PET/CT imaging to search ''enhanced choline influx,'' as worded in the marketing authorization, in hyperfunctioning parathyroid glands was based on recent case reports; its application in parathyroid imaging was considered as potential, but not documented. All patients gave their consent.

Seventeen patients who fulfilled these criteria were referred for FCH-PET/CT before parathyroid surgery, from July 2012 until August 2014, for primary hyperparathyroidism (n = 11), lithium-associated hyperparathyroidism (n = 1), or renal secondary hyperparathyroidism (1 dialyzed patient, 4 transplanted patients); their results were prospectively studied. The results of visual interpretation of FCH-PET/CT of 11 of them has already been reported,[13] but the quantification of FCH uptake and the comparison with the results of US and of ^{99m}Tc-sestaMIBI scintigraphy by open and by masked readings were undertaken for the present study. Twelve patients were female, five patients were male, and their mean age was 52 years (range 25–75). Two patients (#5 and #16) had a history of breast cancer in remission. In all patients, the diagnosis of hyperparathyroidism was based on elevated serum parathyroid hormone (PTH) levels, determined with an immunoradiometric assay for intact PTH (upper limit of normal level = 60 pg/mL). For the single hemodialyzed patients with severe secondary hyperparathyroidism, parathyroidectomy was indicated because of persistently elevated serum levels of intact PTH (mean 1946 pg/mL) associated with hypercalcemia despite medical therapy with calcium, vitamin D (1,25 dihydroxycholecalciferol) supplements, or phosphate binders. Parathyroidectomy was indicated in the 4 patients bearing a renal transplant because of persistently elevated serum levels of intact PTH (mean 118 pg/mL, range 61–167 pg/mL) and prolonged hypercalcemia for more than 1 year after transplantation. Median delay between preoperative FCH-PET/CT and surgery was 18 days (range 4–123).

High-resolution Ultrasonography

Ultrasonography was conducted in the Department of Radiology by an experienced radiologist (MT), the surgeon (SP) being present. The patient was examined in a supine position with the neck hyperextended. High-resolution US was performed using high-frequency linear transducers (7–12 MHz) for cervical examination over a field extending from the angles of the mandible to the sternum notch. The upper mediastinum was studied using an endocavitary probe for retrosternal exploration (4.5–7.2 MHz probe). Transversal and longitudinal views were obtained; images of regions of interest were recorded on film reproducing video images. In addition to identification of the involved parathyroid glands, the thyroid parenchyma was studied. The radiologist was asked to score the presence of hyperplastic parathyroid gland(s) for each possible location (on the right and left sides of the thyroid bed and cervical ectopic glands). Images reported as equivocal were considered as negative in the primary analysis, but the consequences of considering them as positive were also evaluated.

Dual-phase Dual-isotope ^{123}I/^{99m}Tc-sestaMIBI Scintigraphy

All patients underwent dual-phase dual-isotope ^{123}I/^{99m}Tc-sestaMIBI scintigraphy. Oral administration of ^{123}I, 0.1 MBq/kg of body weight, was followed 3 hours later by intravenous administration of ^{99m}Tc-sestaMIBI, 8 MBq/kg. Dual-isotope images were obtained 20 minutes and 3 hours after the intravenous administration of ^{99m}Tc-sestaMIBI. At both phases, a

pinhole collimator was used to image the thyroid bed (10-minute acquisition time), and a parallel hole collimator, to image a large field extending from the salivary glands to the myocardium (7-minute acquisition time). Images of the neck and upper thorax were obtained in planar anterior incidence, with the patient in a supine position and the neck hyperextended. Late (3 hours postinjection) images were used to confirm results of the early phase: the washout of ^{99m}Tc-sestaMIBI is usually quicker in the thyroid gland than in hyperfunctioning parathyroid glands, which therefore become visible with a better contrast over the thyroid gland background. However, this phenomenon is not observed in all cases and was not mandatory to consider a ^{99m}Tc-sestaMIBI-positive focus as corresponding to a hyperfunctioning parathyroid gland. On-site image interpretation was visual from raw images and subtraction of the ^{99m}Tc-sestaMIBI and ^{123}I images, obtained simultaneously at both phases. It was performed by an experienced nuclear medicine physician (JNT). He was asked to score the number of foci evocative of abnormal parathyroid glands in three sites (right and left thyroid beds, and ectopic areas). The number of foci per site could be 0, 1, 2, or even more. Equivocal images could be mentioned; they were considered as negative in the primary analysis, but the consequences of considering them as positive were also evaluated. Images considered to correspond to thyroid nodules should also be mentioned. Masked reading of ^{123}I/^{99m}Tc-sestaMIBI scintigraphy of all patients was performed similarly by another experienced nuclear medicine physician (SB) without any information on patients, including the type of hyperparathyroidism.

18F-fluorocholine PET/CT

A Gemini Dual PET/CT camera (Philips) was used, with low-dose CT (120 kVp, 30–50 mAs) acquired first. Subsequently, with the patient staying inside the tunnel of the PET/CT camera (Philips Gemini TF 16), FCH (3 MBq/kg of body mass) was administered intravenously in an infusion line connected to saline. Immediately after injection, PET dynamic acquisition was performed during 10 minutes with the detector ring centered on the neck, immediately followed by a ''static'' PET acquisition (2 minutes per bed position) ranging from the skull to mid thighs for men (in order not to miss potential prostate foci) and to the lower limit of the liver for women. Dynamic images were also reframed by summing up images from the 2nd to the 8th minute to facilitate interpretation (Figs. 1–4).

Experienced nuclear medicine physicians interpreted on-site FCH-PET/CT images, evaluating visually the number of foci evocative of hyperfunctioning parathyroid glands in 3 sites, as described above. Masked reading of all FCH-PET/CT was performed by another experienced nuclear medicine physician blinded to any information on the patient, including the type of hyperparathyroidism. On the ''static'' PET acquisition, the masked reader also determined the SUVmax of any abnormal focus and the ratio of the SUVmax between the focus and the neighboring thyroid tissue. As the same nuclear medicine specialist (SB) also performed the masked reading of the ^{123}I/^{99m}Tc-sestaMIBI scintigraphy, a wash-out period of at least 1 month was observed between the two sessions of masked reading, with a different randomization of the anonymous data. To further avoid carry-over of information that could favor FCH-PET/CT, the experimental modality, the masked reading of PET/CT was performed as the first session.

Surgery

Results of on-site open readings of US, ^{123}I/^{99m}Tc-sestaMIBI scintigraphy, and FCH-PET/CT were used by the same surgeon to plan and perform surgical interventions. A retrothyroid approach was used. Exploration to search abnormal parathyroid glands was performed under general anesthesia, using a transverse collar incision. Abnormal parathyroid glands were removed (commonly 1 in primary hyperparathyroidism, and 1 or more in secondary hyperparathyroidism). For patient #14, the surgeon decided to limit the intervention to a right parathyroidectomy only, even though imaging modalities described abnormal parathyroid glands on both sides; thus, the abnormal images in the left thyroid bed were not evaluable. Histological analysis of frozen sections was used to confirm the presence of parathyroid tissue. In 7 patients, thyroid gland exploration, hemithyroidectomy, or total thyroidectomy was performed after parathyroidectomy due to suspicious thyroid nodule(s) described preoperatively on imaging modalities.

Histopathological Findings

Three histopathological parameters were gathered to analyze the performance of presurgical imaging: confirmation of parathyroid tissue on frozen sections, definitive histopathological examination, and the weight of removed parathyroid glands. Histological examination of the resected thyroid tissue was performed in cases of hemithyroidectomy or total thyroidectomy.

Statistics

Results of imaging examinations were evaluated, with surgical exploration and histopathological examination of the specimens as the reference standard. We calculated on a per-patient level the sensitivity of each modality (open reading of US, open and masked readings of ^{123}I/^{99m}Tc-sestaMIBI scintigraphy, open and masked readings of FCH-PET/CT). This patient-based sensitivity reflects the proportion of patients in whom at least 1 abnormal parathyroid gland at histology actually corresponded to an abnormal image or focus in the correct site at imaging.

For the per-lesion analysis of each modality, an abnormal image or focus was classified either as a true-positive (TP) result if it corresponded to an abnormal parathyroid gland on the same side of the thyroid bed or in an ectopic position, or as a false-positive (FP) result if it did not. If no abnormal image or focus was reported in a site, the presence of any abnormal gland was considered a false-negative (FN) result; a result was considered true-negative (TN) in a site only if the gland(s) was (were) normal or if no gland was found at surgery.

Sensitivity values for the imaging modalities and types of reading were compared using Mac Nemar test. Due to the small size of the series and the pilot nature of the study, no attempt was made to correct for the clustered nature of some lesion-based data (24 abnormal parathyroid glands in 17 patients).

RESULTS

The results of serum PTH level at the time of FCH-PET/CT, imaging modalities, and histopathological findings are summarized in Table 1.

Surgery and Histopathological Findings on Parathyroid Glands

Parathyroidectomy was performed in all 17 patients. Abnormal parathyroid glands were found in all patients but 1

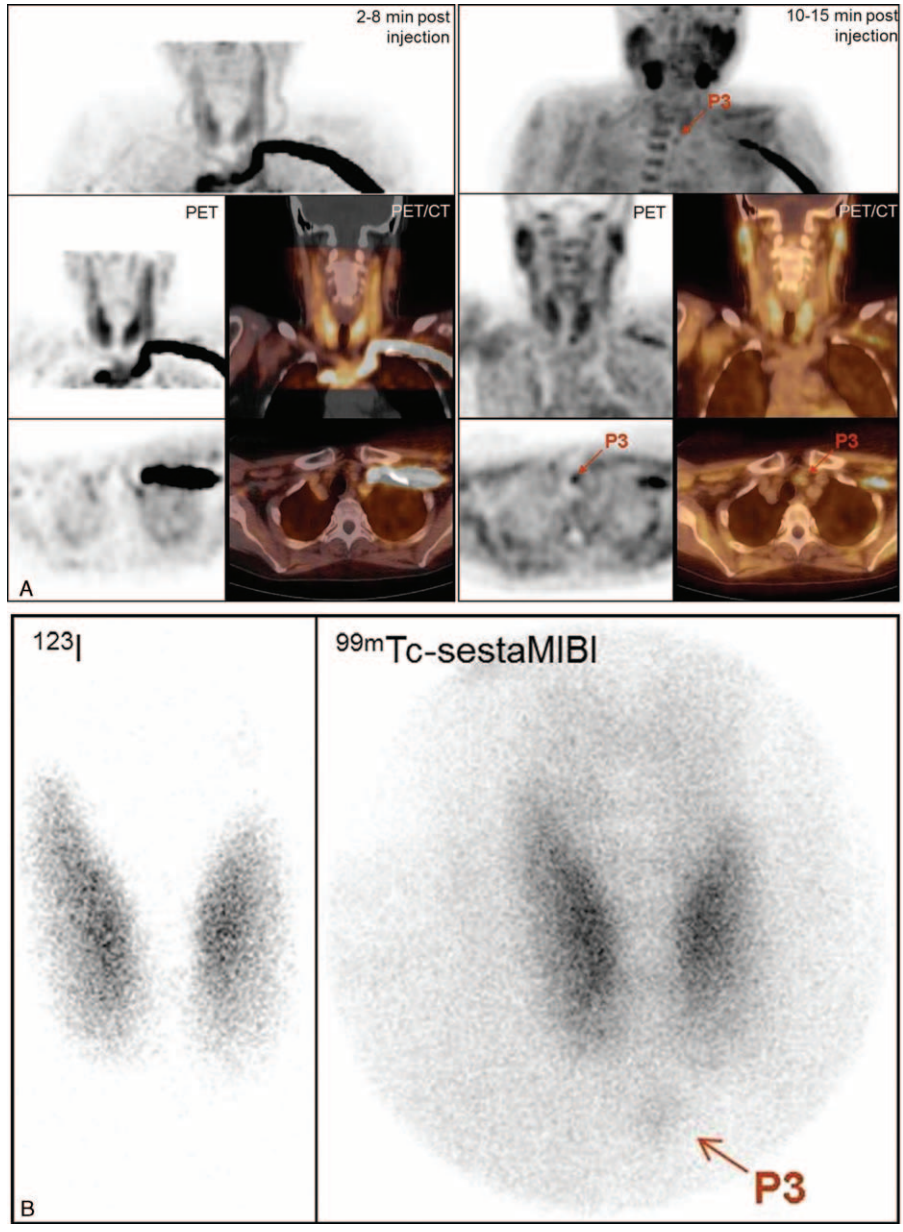

FIGURE 1. Primary hyperparathyroidism (patient #6). A, FCH-PET and PET/CT fused images (MIP, coronal and transversal slices, summed dynamic images in the left column, upper static images in the right column): focus evocative of a left inferior hyperfunctioning parathyroid gland, better visible on the static images. B, $^{123}I/^{99m}Tc$-sestaMIBI scintigraphy: discrete focus evocative of a left inferior hyperfunctioning parathyroid gland. On postsurgical histology, a 0.3 g adenoma was found. PTH serum levels decreased from 70 pg/mL preoperatively to 4 pg/mL on the day after surgery. FCH-PET/CT = ^{18}F-fluorocholine hybrid positron emission tomography/X-ray computed tomography; PTH = parathyroid hormone; sestaMIBI = sesta-methoxyisobutylisonitrile.

(#12), whose hyperparathyroidism was induced by lithium therapy and progressively resolved after discontinuation of treatment, but postsurgical histology actually discovered metastatic thyroid carcinomas and adenomas. This patient #12 was the only negative case for parathyroid pathology; thus, patient-based specificity could not be calculated for the series. Postsurgical histology of parathyroid glands revealed 9 parathyroid adenomas, 15 hyperplastic parathyroid glands, and 5 normal parathyroid glands. Furthermore, 4 sites were explored by the surgeon and no parathyroid gland was found, bringing to 9 the total number of surgically assessed negative sites. The weight of each abnormal parathyroid gland was measured, except for 4 glands in 3 patients (#4, #8, and #14). Overall, it ranged from 0.02 to 5.4 g (median 0.3 g). Weight range was 0.2 to 5.4 g (median 0.4 g) for adenomas and 0.02 to 0.8 g (median 0.2 g) for hyperplastic glands ($P = 0.02$).

PTH Level Preoperatively and at Day 1 Postsurgery

Mean preoperative serum level of PTH was 280 pg/mL, ranging from 61 to 1946 pg/mL. It was 204 pg/mL (range 70–

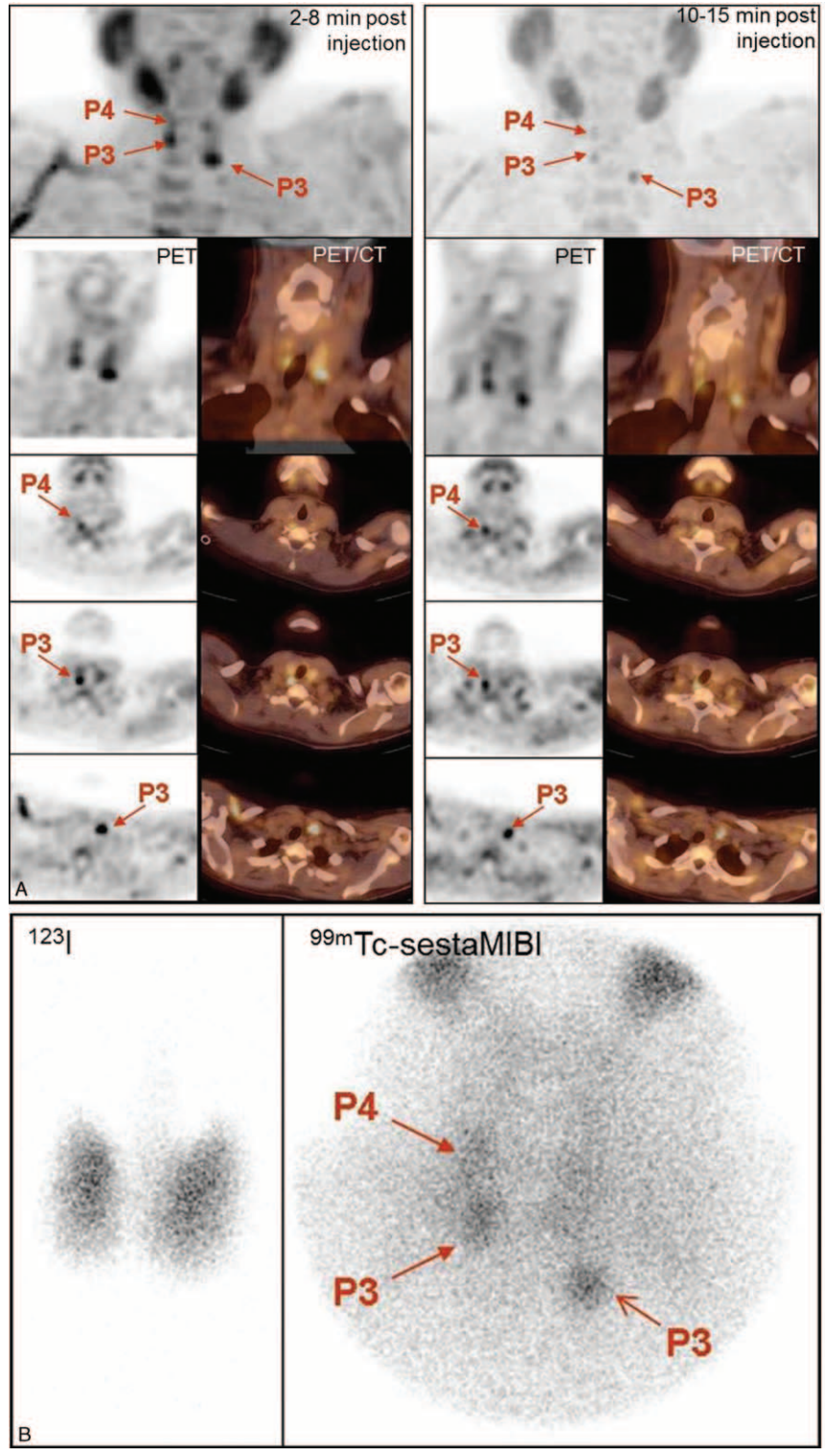

FIGURE 2. Secondary hyperparathyroidism in a dialysed patient (patient #13). A, FCH-PET and PET/CT fused images (MIP, coronal and 3 levels of transversal slices, summed dynamic images in the left column, upper static images in the right column): foci evocative of P3, P4 right, and P3 left hyperfunctioning parathyroid glands, visible on both dynamic and static images. B, $^{123}I/^{99m}Tc$-sestaMIBI scintigraphy: foci evocative of the same 3 hyperfunctioning parathyroid glands. On postsurgical histology, three 0.1 g hyperplastic parathyroid glands corresponding to those foci were found. PTH serum levels decreased from 1946 pg/mL preoperatively to 146 pg/mL on the day after surgery. FCH-PET/CT = ^{18}F-fluorocholine hybrid positron emission tomography/X-ray computed tomography; sestaMIBI = sesta-methoxyisobutylisonitrile.

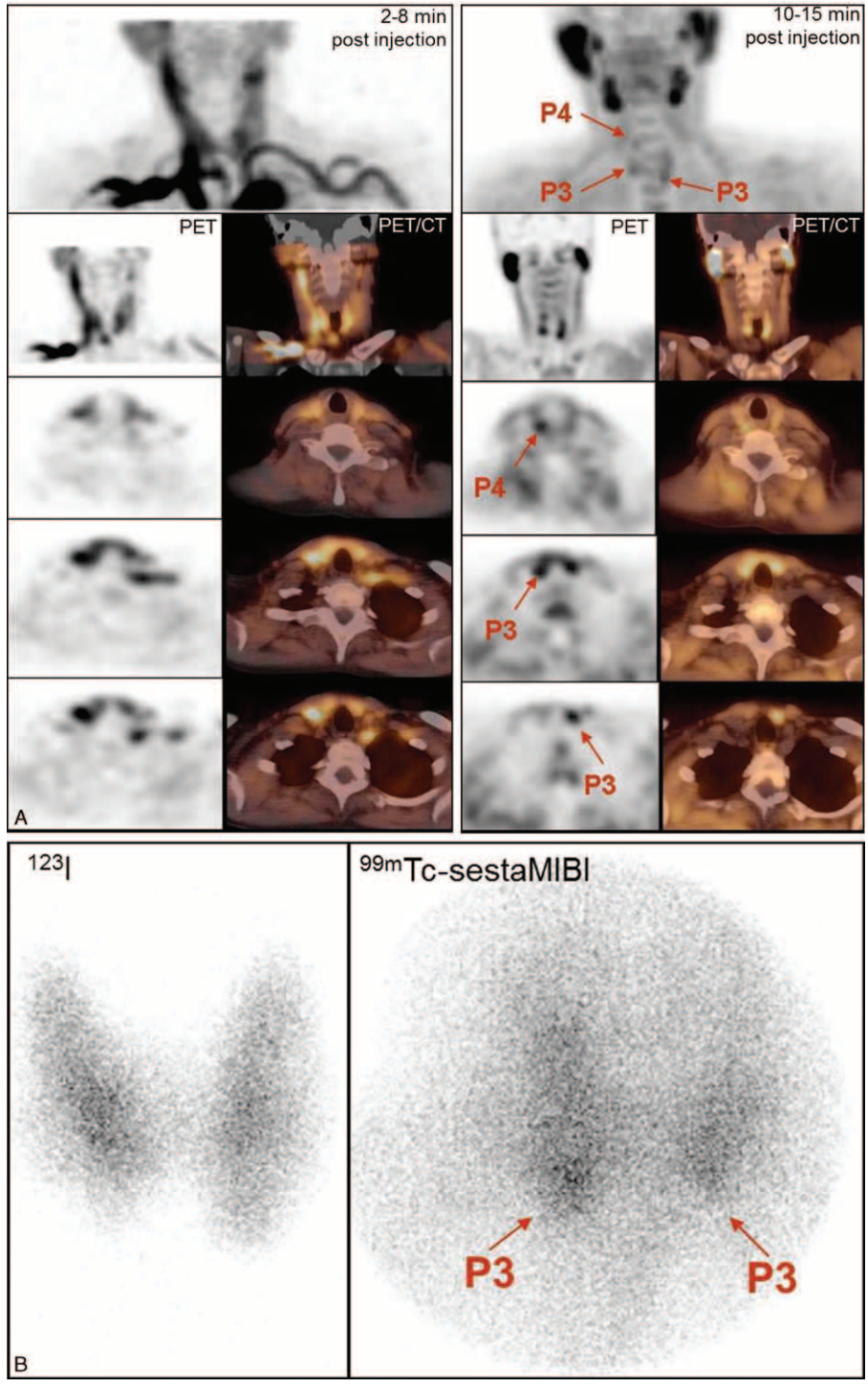

FIGURE 3. Persistent secondary hyperparathyroidism in a patient after renal transplantation (patient #16). A, FCH-PET and PET/CT fused images (MIP, coronal and 3 levels of transversal slices, summed dynamic images in the left column, upper static images in the right column): foci evocative of P3, P4 right, and P3 left hyperfunctioning parathyroid glands, identified only on the static images. B, $^{123}I/^{99m}Tc$-sestaMIBI scintigraphy: discrete focus evocative of a right inferior hyperfunctioning parathyroid gland; on open reading, another discrete focus evocative of a right inferior hyperfunctioning parathyroid gland was also mentioned. On postsurgical histology, three hyperplastic parathyroid glands corresponding to the FCH foci were found, their weight ranging from 0.1 to 0.3 g. PTH serum levels decreased from 167 pg/mL preoperatively to 70 pg/mL on the day after surgery. FCH-PET/CT = ^{18}F-fluorocholine hybrid positron emission tomography/X-ray computed tomography; PTH = parathyroid hormone; sestaMIBI = sesta-methoxyisobutylisonitrile.

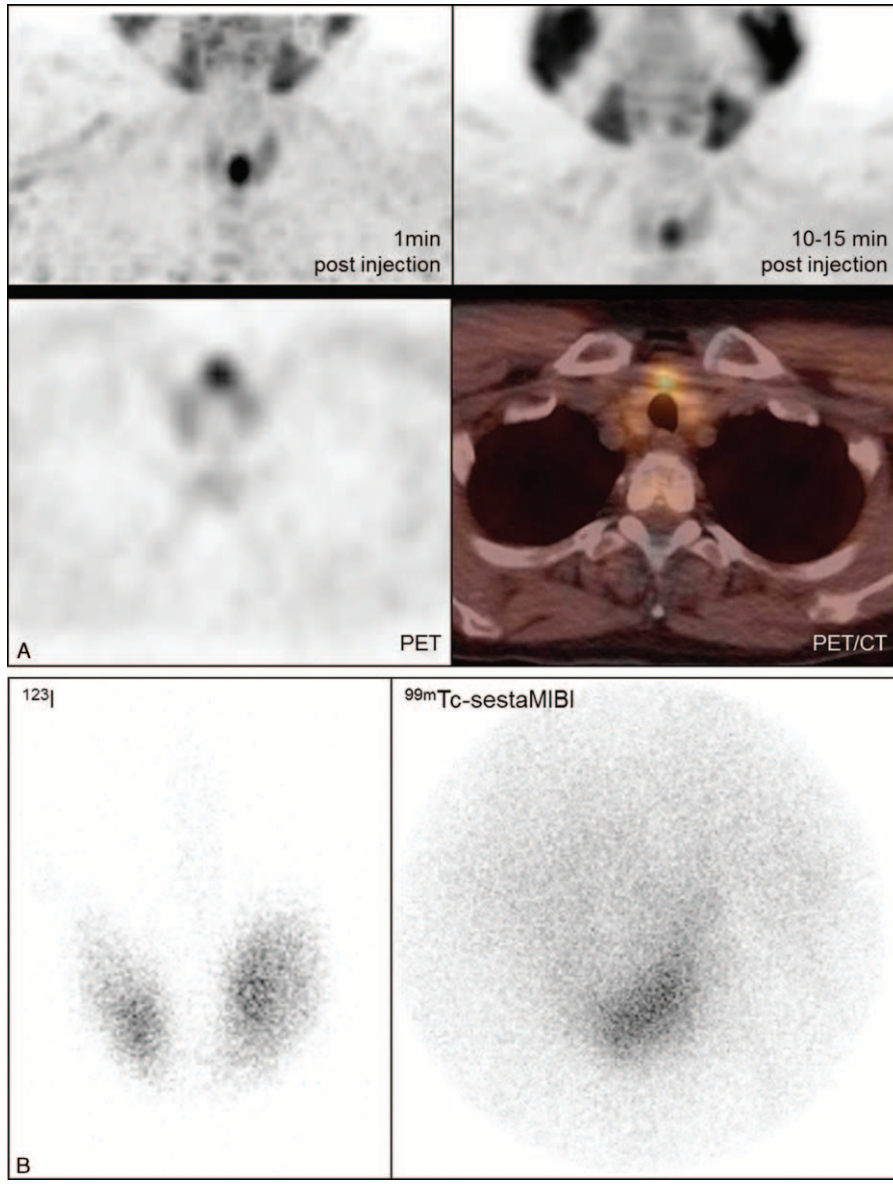

FIGURE 4. Lithium-induced hyperparathyroidism (patient #12). A, FCH-PET and PET/CT fused images (MIP, coronal and transversal slice, early dynamic image in the left column, upper static images in the right column): a large focus with early and intense uptake extending over the thyroid isthmus and the adjacent part of the thyroid left lobe (thyroid nodule or hyperfunctioning parathyroid gland?). B, ^{123}I/^{99m}Tc-sestaMIBI scintigraphy: similar focus corresponding to an iodine-negative part of the thyroid gland. By discontinuing lithium therapy, PTH serum levels decreased from 165 pg/mL to 90 pg/mL at the time of PET/CT and to 40 pg/mL on the day after surgery. This focus actually corresponded to a large oncocytic adenoma and a smaller follicular adenoma of the thyroid. Four small bilateral lesions of thyroid carcinoma with lymph nodes metastases were discovered at histology (all < 2 mm in size), but no abnormal parathyroid gland. FCH-PET/CT = ^{18}F-fluorocholine hybrid positron emission tomography/X-ray computed tomography; PTH = parathyroid hormone; sestaMIBI = sesta-methoxyisobutylisonitrile.

781) in case of primary hyperparathyroidism and 483 pg/mL (range 61–1946) in case of secondary hyperparathyroidism (Table 1). At day 1 postoperatively, PTH serum level decreased in all patients. The median decrease was 77% (from 10% to 99%), the 10% decrease was observed in patient #14 who had only partial parathyroidectomy for secondary hyperparathyroidism; the decrease was greater than 50% or in all other patients (including #12 after stopping lithium therapy).

Patient-based Detection Rate of Imaging Modalities (Tables 1–3)

On a per-patient level, the sensitivity was 38% for US, rising to 50% if equivocal images were to be considered positive. For on-site open reading of ^{123}I/^{99m}Tc-sestaMIBI scintigraphy, it was 69%, rising to 94% if equivocal foci were to be considered positive. For masked reading of ^{123}I/^{99m}Tc-sestaMIBI scintigraphy, it was 94%, without reporting any

TABLE 1. Results of ultrasonography (US), $^{123}I/^{99m}Tc$-sestaMIBI scintigraphy and FCH-PET/CT (open and masked readings), related to surgical and pathological findings

Diagnosis	PTH (pg/mL)	US open-reading	^{99m}Tc-sestamibi/^{123}I open reading	^{99m}Tc-sestamibi/^{123}I masked reading	FCH-PET/CT open reading	FCH-PET/CT masked reading	Surgery and pathological findings
Primary HPT	80	No image of parathyroid gland	Right P3	Right P3	Right P3	Right P4	Ad right P3 (0.4 g)
Primary HPT	200	Left P4	Right P3	Right P4	Right P3 Left P3	Right P3 Left P4	Ad right P3 (1.5 g) Normal left P4 (0.2 g)
Primary HPT	70	Doubt left P3	Left P3	Left P3	Left P3	Left P3	Hp left P3 (0.4 g)
Primary HPT	127	Left P3	Left P3	Right P4	Doubt left P3	Left P3	Hp left P3 (not weighted)
		Doubt right or intrathyroidal P or thyroid nodule	Intrathyroidal right P4		Right and left thyroid nodules		Right (19 mm) and left (17 mm) papillary thyroid carcinoma
			Right and left thyroid nodules				
Primary HPT	94	Doubt P below thyroid isthmus	Doubt P below thyroid isthmus	Left P3	P below thyroid isthmus	P below thyroid isthmus	Ad below thyroid isthmus (1.8 g)
Primary HPT	70	Left P3	Doubt median P3	Left P3	Left P3	Left P3 Left thyroid nodule	Ad left P3 (0.3 g) No left thyroid nodule
Primary HPT	464	Left P	Left P4	Left P4	Left P4	Left P4	Ad left P4 partially intra-thyroidal (5.4 g)
			Left thyroid nodule		Left thyroid nodule	Left thyroid nodule	No left thyroid nodule
Primary HPT	781	Right P3	Right P3	Right P3	No focus evocative of parathyroid gland	Right P3	Ectopic P Ad close to the right recurrent nerve (not weighted)
		Right P4 Left thyroid nonspecific micronodule					No right P3
Primary HPT	80	Doubt right P4 Left thyroid nodule	Left P3	Left P3 Left P4	Left P3 Left thyroid nodule	Left P3	Hp left P3 (0.3 g) Left thyroid carcinoma (papillary-follicular 12 mm)

Diagnosis	PTH (pg/mL)	US open-reading	^{99m}Tc-sestamibi/^{123}I open reading	^{99m}Tc-sestamibi/^{123}I masked reading	FCH-PET/CT open reading	FCH-PET/CT masked reading	Surgery and pathological findings
Primary HPT	143	No image of parathyroid gland	Left P3	Left P3	Left P3	Left P3	Ad left P3 (0.3 g), normal left P4
			Doubt right P3				
Primary HPT	140	Left P3	Left P3	Left P3	Left P3 Doubt right P3	Left P3	Ad left P3 (0.2 g)
Lithium-induced HPT	90	Doubt left P or left thyroid nodule	Doubt left P or left thyroid nodule	Left P3	Left thyroid nodule	Left P3	Normal right P (8 mm), 2 left thyroid adenomas (1 oncocytic 3.5 g, 1 follicular 10 mm), 4 bilateral foci of papillary thyroid carcinoma all $\leq$2 mm and lymph node metastases
Secondary HPT (dialyzed)	1946	No image of parathyroid gland	Right P3	Right P3	Right P3	Right P3	Hp right P3 (0.1 g)
			Right P4	Right P4	Right P4	Right P4	Hp right P4 (0.1 g)
			Left P3	Left P3	Left P3	Left P3	Hp left P3 (0.1 g)
Secondary HPT (grafted)	61	No image of parathyroid gland	Doubt right P4	Right P3	2 right P3 Right P4	Right P3	Right parathyroidectomy only
		Nonspecific thyroid nodules		Right P4	Left P3	Right P4	Hp right P3 (not weighted)
				Left P3	Left P4	Left P3	Hp right P4 (not weighted)
				Left P4		Left P4 Left thyroid nodule	
Secondary HPT (grafted)	110	Right P4	Left P4	Left P4	Left P4	Right P4	Ad left P4 (0.4 g)
			Doubt right P4			Left P4	No detectable right parathyroid gland
Secondary HPT (grafted)	167	Right P3	Right P3	Right P3	Right P3	Right P3	Hp right P3 (0.1 g)
		Right P4	Left P3		Right P4	Right P4	Hp right P4 (0.3 g)
		Left P3			Left P3	Left P4	Hp left P3 (0.2 g)
		Multinodular goiter					Multinodular right thyroid lobe, no cancer

Diagnosis	PTH (pg/mL)	US open-reading	^{99m}Tc-sestamibi/^{123}I open reading	^{99m}Tc-sestamibi/^{123}I masked reading	FCH-PET/CT open reading	FCH-PET/CT masked reading	Surgery and pathological findings
Secondary HPT (grafted)	132	Right P3	Doubt right P3	Right P3	Right P3	Right P3	Hp right P3 (0.4 g)
		Right P4	Doubt left P3	Right P4	Left P3	Right P4	Hp right P4 (0.2 g)
		Left P3	Left P4	Left P3	Left P4	Left P3	Hp left P3 (0.02 g)
		Right thyroid nodule		Left P4	Doubt intrathyroidal right P4 or right thyroid nodule	Left P4	Hp left P4 (0.8 g)
							Right thyroid nodule including two papillary carcinomas (5 mm each)

Ad = parathyroid adenoma; Hp = hyperplastic parathyroid gland (dimension corresponds to long axis); HPT = hyperparathyroidism; P = parathyroid gland; P3 = inferior P; P4 = superior P.

doubtful focus. For on-site open reading of FCH-PET/CT, it was 88%, rising to 94% if equivocal foci were to be considered positive. For masked reading of FCH-PET/CT, the detection rate was 94%, without reporting any equivocal focus. US sensitivity was inferior to that of FCH-PET/CT (all readings $P < 0.03$) and of scintigraphy if equivocal foci were to be considered positive ($P < 0.02$). In masked reading, the sensitivity was identical for scintigraphy and FCH-PET/CT, and was not significantly different from that of open reading (all $P > 0.1$).

Lesion-based Diagnostic Performance of Imaging Modalities

The analysis was first performed considering as negative the images or foci reported as equivocal (Table 2). On a per-lesion level, US sensitivity was 42% and specificity 67%. The lesion-based sensitivity of open reading of ^{123}I/^{99m}Tc-sesta-MIBI scintigraphy was 58% and specificity 78%; in masked reading, the corresponding values were 83% and 56%, respectively. Lesion-based sensitivity and specificity of open reading of FCH-PET/CT were both 88%; for masked reading, the corresponding values were 96% and 56%, respectively.

When considering the equivocal images or foci as positive (Table 3), only the diagnostic performance of open reading changed, since the masked reader did not quote any focus as equivocal: sensitivity increased and specificity decreased, but only for US and scintigraphy. On-site reading of FCH-PET/CT considering the equivocal foci as positive had the best lesion-based accuracy of 94%. Lesion-based sensitivity would be significantly inferior for US than for FCH-PET/CT (all $P < 0.01$) or scintigraphy if equivocal foci were to be considered positive ($P = 0.04$). Sensitivity was significantly greater for FCH-PET/CT than for scintigraphy ($P = 0.04$), but only for open reading, if equivocal foci were considered as negative. The difference was not significant in open reading if equivocal foci were considered as positive ($P > 0.2$) or in masked reading (all $P > 0.2$).

There was no significant difference between the sensitivity of open and masked readings of the same imaging modality (all $P > 0.1$).

Concerning lesion-based specificity, no difference reached the level of significance, with only 9 surgically proven negative sites.

False Results of FCH-PET/CT

In patient #8, no focus evocative of a parathyroid gland was reported on on-site open reading of FCH-PET/CT and the ectopic adenoma was not found on any imaging modality: it was actually found at histology in the specimens of the right recurrent basin dissection. In patient #4, a FCH focus was actually reported in the correct localization, but was interpreted on-site as only equivocal, similarly to the 4th hyperplastic parathyroid gland of patient #17. In patient #12 who received lithium therapy, imaging was performed in search for parathyroid hyperplasia or even adenomas.[22,23] A clearly abnormal image on US and a very active focus on scintigraphy and FCH-PET/CT were found (Fig. 4) and the patient was operated. Postsurgical histology of this lesion corresponded to an oncocytic thyroid adenoma (3.5 g), with a smaller follicular adenoma, but no abnormal parathyroid glands; furthermore, 2 very small adenocarcinomas were also discovered on both sides of the thyroid gland with subcentimeter metastatic lymph nodes.

TABLE 2. Performance of each imaging modality for detecting hyperfunctioning parathyroid glands, equivocal images, or foci considered as negative

	Patient-based sensitivity	Lesion-based sensitivity	Lesion-based specificity	Lesion-based accuracy
US open reading	6/16 = 38%	10/24 = 42%	6/9 = 67%	16/33 = 48%
^{99m}Tc-sestamibi/^{123}I open reading	11/16 = 69%	14/24 = 58%	7/9 = 78%	21/33 = 64%
^{99m}Tc-sestamibi/^{123}I masked reading	15/16 = 94%	20/24 = 83%	5/9 = 56%	25/33 = 76%
FCH-PET/CT open reading	14/16 = 88%	21/24 = 88%	8/9 = 88%	29/33 = 88%
FCH-PET/CT masked reading	15/16 = 94%	23/24 = 96%	5/9 = 56%	28/33 = 85%

For patient-based sensitivity, a result was true-positive if at least 1 abnormal image or focus corresponded to 1 abnormal parathyroid gland in the same site of the patient. FCH-PET/CT = ^{18}F-fluorocholine hybrid positron emission tomography/X-ray computed tomography.

Another FP result occurred in patient #2: a left superior parathyroid gland was interpreted as adenomatous on US and hyperfunctioning on open and on masked readings of FCH-PET/CT; this parathyroid gland was surgically explored and histologic examination concluded to a normal parathyroid gland. The other FP results were only noted on one of the readings of FCH-PET/CT. In patient #14, 2 foci were interpreted as abnormal right P4 and 1 as abnormal right inferior parathyroid gland on open reading of FCH-PET/CT; the right thyroid bed was surgically explored and histological examination found just 2 abnormal parathyroid glands. In patient #8 who had one single ectopic adenoma, a right inferior parathyroid gland was interpreted as adenomatous on US and hyperfunctioning on both readings of ^{123}I/^{99m}Tc-sestaMIBI scintigraphy and of masked reading of FCH-PET/CT; the right thyroid bed was surgically explored and histological examination did not find any parathyroid gland. In patient #15, a right superior parathyroid gland was interpreted as hyperplastic on US and hyperfunctioning on open reading of ^{123}I/^{99m}Tc-sestaMIBI scintigraphy and on masked reading of FCH-PET/CT; however, the surgeon explored the right thyroid bed and did not find any abnormal parathyroid gland.

Detection of Anomalies in the Thyroid Gland and in Other Organs

Thyroid nodules were described or suspected on morphological or functional imaging in 9 patients. In 4 of them (#4, #9, #12, and #17), a thyroid carcinoma was found. Thyroid nodules/lesions had been described on US (#4, #12, and #17) or on open reading of sestaMIBI scintigraphy (#4 #12) or of FCH-PET/CT (#4, #9, and #12). As already reported, patient #12 had very small bilateral thyroid cancers with metastatic lymph nodes missed by all imaging modalities, a large oncocytic adenoma that took up intensely sestaMIBI and FCH, and a smaller follicular adenoma. For patient #16, multinodular goiter was described only on US; hemithyroidectomy was decided during the intervention by the surgeon because this lobe actually seemed nodular; there was no thyroid cancer, but abnormal parathyroid glands were removed that had been missed on sestaMIBI imaging. In patient #6, the masked reader quoted a thyroid nodule on FCH-PET/CT, which was not confirmed after hemithyroidectomy. In patient #7, the actual parathyroid adenoma was located inside the left thyroid lobe and was misinterpreted as a thyroid nodule on US and on masked reading of ^{123}I/^{99m}Tc-sestaMIBI scintigraphy. In patients #8 and #14, thyroid nodules were described on imaging modalities, but thyroid surgery was not performed.

In our series, no abnormal FCH focus was visible out of the thyroid bed, in particular, in the prostate of the 5 men or in the breast of the 12 women or in the liver of any patient: no prostate cancer or (recurrent) breast cancer or hepatocellular carcinoma was thus discovered as incidentaloma in our series.

Early Dynamic Images

It was noted by the on-site and the masked readers that all the abnormal foci detected on the static PET acquisition started 10 minutes after FCH injection was already visible on the early dynamic PET acquisition, even though the significant activity

TABLE 3. Performance of each imaging modality for detecting hyperfunctioning parathyroid glands, equivocal images, or foci considered as positive

	Patient-based sensitivity	Lesion-based sensitivity	Lesion-based specificity	Lesion-based accuracy
US open reading	8/16 = 50%	12/24 = 50%	3/9 = 33%	15/33 = 46%
^{99m}Tc-sestamibi/^{123}I open reading	15/16 = 94%	20/24 = 83%	5/9 = 56%	25/33 = 76%
^{99m}Tc-sestamibi/^{123}I masked reading	15/16 = 94%	20/24 = 83%	5/9 = 56%	25/33 = 76%
FCH-PET/CT open reading	15/16 = 94%	23/24 = 96%	8/9 = 88%	31/33 = 94%
FCH-PET/CT masked reading	15/16 = 94%	23/24 = 96%	5/9 = 56%	28/33 = 85%

For patient-based sensitivity, a result was true-positive if at least one abnormal image or focus corresponded to one abnormal parathyroid gland in the same site of the patient. When an image was interpreted as equivocal for either an abnormal parathyroid gland or a thyroid nodule, the actual presence of a thyroid nodule was not considered as a false-positive result. FCH-PET/CT = ^{18}F-fluorocholine hybrid positron emission tomography/X-ray computed tomography.

of the tracer in the blood vessels imposed a more careful analysis of the cross-sectional images (Figs. 1–4). Furthermore, no abnormal focus was visible on the dynamic images that disappeared on the subsequent static images.

Quantification of FCH Uptake in Foci Detected on Masked Reading

The SUVmax values of the 23 abnormal parathyroid glands detected on FCH-PET/CT ranged from 2.4 to 11.9 (mean 3.9, median 3.1). Its ratio with the SUVmax of neighboring thyroid tissue ranged from 0.85 to 3.7 (mean 1.5, median 1.2). The ratio was >1 for 17/23 (74% of the glands), including 6/8 adenomas. A trend to a greater FCH uptake by adenomas (mean SUVmax 4.6, mean ratio 1.82) than by hyperplastic glands (mean SUVmax 3.5, mean ratio 1.26) was observed, but did not reach the level of statistical significance. Correlation between FCH uptake and PTH serum level was not significant. The same measurements were performed on 5 thyroid lesions that were visible on PET/CT. The SUVmax and SUVmax ratio were similar for 2 carcinomas and 2 adenomas (range SUVmax 2.5–3.3, ratio 0.97–1.28), and similar to those of hyperplastic parathyroid glands; a far greater uptake by the oncocytic adenoma of patient #12 was observed (SUVmax 9.5, ratio 1.86) (Fig. 4).

DISCUSSION

This pilot study was prompted by the incidental discovery of hyperfunctional parathyroid glands on FCH-PET/CT of 2 patients referred to our center for imaging of prostate cancer.[3] We deliberately submitted a series associating different types of hyperparathyroidism to the readers. This was meant to avoid an interpretation bias which probably occurred in studies limited to primary hyperparathyroidism. In patients with primary hyperparathyroidism, only 1 focus is expected to be found at imaging and a specific reading on the per-lesion level is favored, whereas 4 foci are expected in patients with secondary hyperparathyroidism which favors a sensitive but less specific interpretation. The association of different types of hyperparathyroidism in the series aimed to favor a balanced reading, in particular, masked reading.

We[13] and others[11,12] confirmed that FCH uptake is a general property in case of adenomatous or hyperplastic parathyroid glands[11,13] in non-cancer patients, independently of the type of hyperparathyroidism, either primary (Fig. 1)[11–13] or secondary (Figures 2 and 3).[13] In the present series, abnormal parathyroid glands (9 adenomas and 15 hyperplastic glands) were detected on FCH-PET/CT by the masked reader in all patients, but 1 who had 1 ectopic cervical parathyroid adenoma was missed by all imaging modalities. Most of the abnormal parathyroid glands detected on FCH-PET/CT weighted 0.1 g or more and their long axis was greater than 10 mm, but in patient #17, the hyperplastic gland only weighted 0.02 g, with a 5-mm long axis.

Moreover, FCH-PET/CT yielded a significantly better diagnostic performance than US, both being read on-site, as masked reading was not possible for US. There was a trend for a better sensitivity of FCH-PET/CT compared with dual-phase dual-isotope scintigraphy, but the difference was significant only in lesion-based sensitivity for open reading, the doubtful results being considered as negative ($P = 0.04$). For masked reading (which proved to be performed in a sensitive manner), the difference did not reach the level of significance.

In 2014, Lezaic et al[11] published the results of another pilot study comparing FCH-PET/CT and ^{99m}Tc-sestaMIBI imaging. Their study sample (21 adenomas and 18 hyperplastic parathyroid glands in 24 patients) was somewhat larger than ours (9 adenomas and 15 hyperplastic parathyroid glands in 17 patients), but was limited to patients with primary hyperparathyroidism and no anomaly of the thyroid gland. The median weight of the abnormal glands was exactly the same as in our series, the smallest detected abnormal gland being, however, lighter in our series (0.02 g vs 0.1 g). Overall, lesion-based sensitivity of FCH-PET/CT was 92% in the study by Lezaic et al, which is significantly greater than the values for ^{99m}Tc-sestaMIBI imaging, which ranged from 44% to 64% according to the acquisition protocol (^{99m}Tc-sestaMIBI SPECT/CT alone, single isotope thyroid subtraction, dual-phase acquisition, or combined). Therefore, these results are in complete accordance with ours concerning the high diagnostic performance of FCH-PET/CT in primary hyperparathyroidism. The superiority of FCH-PET/CT over ^{99m}Tc-sestaMIBI imaging was more definite in the study by Lezaic et al because the performance of ^{99m}Tc-sestaMIBI imaging was somewhat lower than in our study: the best value for sensitivity was 64% for the centralized reading of the combined method versus 83% for masked reading of dual-phase dual-isotope scintigraphy in our series. This may be due to the dual-isotope method that we used, which allows simultaneous acquisition of ^{123}I and ^{99m}Tc-sestaMIBI images, resulting in a better delineation of the thyroid gland and in reducing the consequences of movements of the patient. The influence of the protocol used for parathyroid scintigraphy as the comparator will be discussed below, among the limitations of our study.

In a conference abstract, results of another series were reported on FCH-PET/CT in primary hyperparathyroidism.[12] Out of 15 patients with negative or equivocal ^{99m}Tc-sestaMIBI imaging, FCH-PET/CT detected abnormal foci in 13; at the time of the abstract publication, surgery was only performed in 3 patients and confirmed PET/CT findings. The mean SUV in lesions was 5.0 (range 3.0–9.2), which is similar to the SUVmax values that we measured in adenomas (mean 4.6, range 2.4–11.9).

The pilot study of Orevi et al[10] in 2014 compared ^{11}C-choline PET/CT with ^{99m}Tc-sestaMIBI imaging in primary hyperparathyroidism. In 23 cases, both ^{11}C-choline and ^{99m}Tc-sestaMIBI matched surgical findings of parathyroid adenoma. In 1 case, parathyroid adenoma was correctly localized with ^{11}C-choline, but not with ^{99m}Tc-sestaMIBI, and in 2 cases, neither ^{11}C-choline nor ^{99m}Tc-sestaMIBI corresponded to the surgical findings.

In summary, according to concordant results of the 4 pilot studies using 2 different radionuclides, sensitivity of choline-based PET/CT in detecting abnormal parathyroid glands is at least as high as that of ^{99m}Tc-sestaMIBI scintigraphy or single-photon emission computed tomography (SPECT)/CT.

In our study, the definition of a negative site, and that of a positive site, was based on surgery and histology. This is different from other studies which accepted persistence of normal PTH serum levels after surgery as evidence to consider as negative sites that have not been surgically explored. FP and FN results were frequently due to misinterpretation of thyroid anomalies (Table 1). The other studies did not highlight this interference.

It was not possible to differentiate abnormal parathyroid glands from thyroid lesions based on SUVmax of the focus or its ratio to SUVmax of normal thyroid tissue. Abnormal

parathyroid glands (26%), including some adenomas, had a lower uptake than the normal thyroid tissue. In our series, thyroid anomalies were suspected on imaging in 9/17 (53%) of patients referred for hyperparathyroidism and were confirmed in 6 of the 7 patients who underwent thyroidectomy. This large proportion may be explained by the recruitment based on equivocal results of US or scintigraphy, which are more frequent in case of anomalies of the thyroid gland.[18–20] Thyroid cancer was found in 4/17 (24%) of the patients. Such a proportion of thyroid cancers has already been observed in case of hyperparathyroidism.[27,28] We previously reported that a 45 mm papillary carcinoma appeared as an incidental FCH focus in the thyroid gland[3]; a high FCH uptake by a large B-cell lymphoma infiltrating the left thyroid lobe has also been published.[29] In the present series, only 2 nodules corresponding to thyroid carcinoma were detected on dual-isotope ^{123}I/^{99m}Tc-sestaMIBI scintigraphy versus 3 on FCH-PET/CT; their contrast with FCH uptake of normal thyroid tissue was not greater than that of a typical follicular adenoma of thyroid gland or of a hyperplastic parathyroid gland. The 6 cancer lesions missed on FCH-PET/CT were 5 mm or less in long axis. An oncocytic thyroid adenoma containing oxyphilic cells intensely took up sestaMIBI and FCH. We already described such intense uptake of FCH and FDG by an oncocytic adenoma in a patient referred to PET/CT for recurrent hepatocholangiocarcinoma.[6]

Compared with dual-isotope ^{123}I/^{99m}Tc-sestaMIBI scintigraphy, the disadvantage of FCH-PET/CT is its lack of tracer taken up by normal thyroid tissue. Dual tracer simultaneous acquisition is not possible with PET. The differential diagnosis between thyroid and parathyroid anomalies is thus based on topographic criteria in fused PET/CT images. Associating PET/CT with the US images of thyroid parenchyma seems efficient.

In contrast, PET has advantages over scintigraphy or SPECT. A practical advantage for patients and nuclear medicine centers is the shorter duration of the whole imaging procedure. Indeed, with a time-of-flight PET/CT machine like ours,[30] total duration of image acquisition was 10 minutes for dynamic PET and 25 minutes for the subsequent static acquisition. Actually the dynamic acquisition brought no further information as compared to the static acquisition. In the present series, no unexpected malignancy out of the thyroid bed which could justify an extensive field of view was discovered. The field of view of the static acquisition could be significantly shortened from the salivary glands to the myocardium, reducing its duration to 10 minutes. We did not perform another PET acquisition 1 hour postinjection.

This was done by Lezaic et al,[11] who observed that all lesions were visible at both imaging times (5–9 minutes and 60–64 minutes postinjection), with visually better lesion-to-background and lesion-to-thyroid contrast on delayed imaging. In our series, one single PET image acquisition over a limited field of view, started just 10 minutes after injection, permited an effective localisation of abnormal parathyroid glands with a limited occupation of the machine and mobilisation of the patient.

The main advantage of PET is a greater spatial resolution of images than scintigraphy or SPECT, but an appropriate and available PET tracer is also needed in routine practice to achieve superior diagnostic performance. Concerning availability, an industrial preparation of FCH has been registered in 2010 in France, and it is used in some PET centers on a routine basis, but FDG is still more widely available. Variable results have been reported with FDG-PET in the detection of adenoma or hyperplastic parathyroid glands: a very low sensitivity in two short series[31,32] or, in comparison with ^{99m}Tc-sestaMIBI, a better sensitivity for detection of parathyroid adenoma (86% vs 43%), but a lower specificity (78% vs 90%).[33] In 2014, Chicklore et al[34] compared FDG and ^{11}C-methionine PET/CT performed in 43 patients referred for hyperparathyroidism of whom only 16 had parathyroid surgery; results favored the amino acid ^{11}C-methionine. ^{11}C-methionine has been considered as the PET alternative for the detection of parathyroid adenomas, with a pooled patient-based sensitivity and detection rate of 81% and 70% according to a recent meta-analysis.[35] An analog of another amino acid, 18F-fluorodihydroxyphenylalanine (FDOPA) has been registered since 2006 in France and is currently available, but it is not effective to detect hyperfunctioning parathyroid glands.[36,37] In contrast, ^{11}C-choline could be an alternative to FCH.[1,10] However, logistics of ^{11}C-labeled tracers are very demanding due to its short 20-minute half-life, requiring the presence of a cyclotron close to the PET center, and their routine use is currently limited to few centers in Europe. FCH would be easier to develop as a parathyroid imaging agent. Its only disadvantage, compared to ^{11}C-choline or ^{11}C-methionine, is its less favorable dosimetry. Nevertheless, the effective dose from FCH administration is not far from that of ^{99m}Tc-sestaMIBI, and is being reduced—thanks to the recent improvement in PET detection.

Our pilot study has some limitations when comparing FCH-PET/CT with US and sestaMIBI imaging. Many patients were recruited because of discrepant results between preoperative US and ^{123}I/^{99m}Tc-sestaMIBI dual-phase scintigraphy, which could explain lower per-patient detection rates and lower sensitivities for US and scintigraphy, since one of the imaging modalities at least had to be wrong. Nevertheless, the superiority of FCH-PET/CT was also obvious in the other pilot study by Lezaic et al,[11] which ignored this inclusion criterion. Concerning abnormal parathyroid glands in an ectopic location in the neck, only 1 was observed in our series, which was missed by all imaging modalities, and none was reported in the other series of FCH-PET/CT.[11,12] As our patient sample was small, no extracervical abnormal glands were found, so the ability of FCH-PET/CT to detect ectopic parathyroid glands has not been tested. Nevertheless, the detection of 1 incidental ectopic parathyroid hyperplasia with FCH has already been reported.[4] One can expect that FCH-PET/CT will be superior in detecting ectopic glands than standard US, which is not performing well in the upper mediastinum, and also than scintigraphy or SPECT due to the better resolution of PET imaging.

Another technical point which may seem as a limitation is that we used planar dual-isotope dual time point scintigraphy instead of SPECT/CT—a cross-sectional imaging modality, limiting the validity of the comparison with PET/CT. In fact, the assessment of a novel imaging technique requires the reference technique to be performed using the protocol that yields the best diagnostic performance. For parathyroid scintigraphy, very variable protocols are still in use, combining single or dual tracer and, in case of dual tracer, single or dual isotope, single or dual time point, planar imaging using pinhole, and/or parallel hole collimator and/or SPECT or SPECT/CT. A recent survey showed that the 19 hospitals performing parathyroid scintigraphy in Finland used 18 different study protocols, the most frequently preferred technique (11/19 hospitals) being the dual-tracer ^{123}I/^{99m}Tc-sestaMIBI that we used.[38] In the version 4.0 of the ''Practice Guidelines for parathyroid scintigraphy'' issued in 2012 by the Society of Nuclear Medicine (SNM), all those techniques are reviewed and the conclusion is: ''None of the preceding techniques has been shown to be diagnostically

superior.''[39] A recent comparative study of several protocols showed that dual-isotope techniques yield a better sensitivity as compared with single-isotope scintigraphy (77–80% vs 13–32%, respectively).[24] To the best of our knowledge, only two studies in the literature compared the dual-isotope technique versus ^{99m}Tc-sestaMIBI SPECT/CT. According to Schalin-Jantti et al,[25] the lesion-based accuracy was far better with the dual-isotope technique (59%) than with SPECT/CT (19%). But according to Hassler et al,[26] the sensitivity was 75% for the dual-isotope technique versus 86% for SPECT/CT, specificity being 90% and 100% respectively. From these recent and conflicting results, it can be concluded, in accordance with the SNM Guidelines,[39] that the protocol of parathyroid scintigraphy used in the present study cannot be considered as suboptimal.

Finally, concerning the potential mechanism of FCH uptake by hyperfunctioning parathyroid glands, we[5] and others postulated the enhancement of a metabolic process: intracellular transport and upregulation of choline kinase to allow membrane accretion of the proliferating tumor cells. Such increased choline kinase activity has been found not only in malignancies but also in adenomas of the colon.[40] Furthermore, this mechanism may be reinforced by the effect of the positive electric charge of FCH, similar to that of sestaMIBI. This positive electric charge is recognized to play a major role in the elective accumulation of sestaMIBI in the mitochondria of the oxyphilic cells, the overexpression of which is necessary to detect the hyperfunctioning parathyroid glands on sestaMIBI scintigraphy.[41,42] This hypothesis is reinforced by the high FCH uptake, as intense as in parathyroid adenomas, observed in oncocytic thyroid adenomas also constituted of oxyphilic cells (1 case in the present series and 1 in our previous series in liver cancer).[6]

Such an amplifying ionic mechanism could in future favor the use of FCH rather than FDG or amino acid tracers for PET imaging of hyperparathyroidism.

CONCLUSION

Results of this pilot series in 17 patients show that FCH-PET/CT can detect abnormal parathyroid glands (adenomatous or hyperplastic glands) in secondary hyperparathyroidism, and also in primary hyperparathyroidism. Moreover, it detected a significantly greater number of abnormal parathyroid glands than US and was at least as sensitive as ^{123}I/^{99m}Tc-sestaMIBI dual-phase scintigraphy without reducing specificity. The early dynamic images acquired just after injection of FCH-PET/CT did not add information compared to static imaging started 10 minutes after injection. One single static acquisition on a limited field of view will correspond to a very short duration of the PET/CT examination, as compared with scintigraphy and even with US. Semiquantification of the FCH uptake by foci did not permit to help visual interpretation in differentiating hyperplastic parathyroid glands from thyroid adenomas and cancers; a trend to a higher FCH uptake in case of parathyroid adenoma or oncocytic adenoma was noted. So it seems that a very simple and uniform imaging protocol could be proposed for FCH-PET/CT in case of hyperparathyroidism, which will contrast with the large variety of protocols that are currently used for ^{99m}Tc-sestaMIBI scintigraphy across centers. Standardized FCH-PET/CT practice will favor the diffusion of this technique. The concordance of the results of our pilot study and of a few others showing a promising diagnostic performance of FCH in this setting warrants conducting a prospective multicenter trial to assess FCH as the functional PET tracer in case of hyperparathyroidism, complemented by US for a better differential diagnosis between abnormal parathyroid glands and concomitant thyroid anomalies. Assessment of the clinical impact of FCH-PET/CT was not an objective of our retrospective pilot study. Future studies should also incorporate a prospective determination of the impact rate of this new modality on the patient management, including surgical procedure, and the verification of the adequacy of the induced changes by following up the patients over several months.

REFERENCES

1. Mapelli P, Busnardo E, Magnani P, et al. Incidental finding of parathyroid adenoma with 11C-choline PET/CT. *Clin Nucl Med.* 2012;37:593–595.
2. Quak E, Lheureux E, Reznik S, et al. F18-Choline, a novel PET tracer for parathyroid adenoma? *J Clin Endocrinol Metab.* 2013;98:3111–3112.
3. Hodolic M, Huchet V, Balogova S, et al. Incidental uptake of 18Ffluorocholine (FCH) in the head or in the neck of patients with prostate cancer. *Radiol Oncol.* 2014;48:228–234.
4. Cazaentre T, Clivaz F, Triponez F. False-positive result in 18F-fluorocholine PET/CT due to incidental and ectopic parathyroid hyperplasia. *Clin Nucl Med.* 2014;39:e328–e330.
5. Kwee SA, DeGrado TR, Talbot JN, et al. Cancer imaging with fluorine-18-labeled choline derivatives. *Semin Nucl Med.* 2007;37:420–428.
6. Talbot JN, Fartoux L, Balogova S, et al. Detection of hepatocellular carcinoma with PET/CT: a prospective comparison of 18F-fluorocholine and 18FFDG in patients with cirrhosis or chronic liver disease. *J Nucl Med.* 2010;51:1699–1706.
7. http://base-donnees-publique.medicaments.gouv.fr/affichageDoc.php?specid=65884187&typedoc=R.
8. Calabria F, Chiaravalloti A, Schillaci O. 18F-choline PET/CT pitfalls in image interpretation: an update on 300 examined patients with prostate cancer. *Clin Nucl Med.* 2014;39:122–130.
9. Balogova S, Huchet V, Kerrou K, et al. Detection of bronchioloalveolar cancer by means of PET/CT and 18F-fluorocholine, and comparison with 18Ffluorodeoxyglucose. *Nucl Med Commun.* 2010;31:389–397.
10. Orevi M, Freedman N, Mishani E, et al. Localization of parathyroid adenoma by 11C-choline PET/CT: preliminary results. *Clin Nucl Med.* 2014;39:1033–1038.
11. Lezaic L, Rep S, Sever MJ, et al. 18F-Fluorocholine PET/CT for localization of hyperfunctioning parathyroid tissue in primary hyperparathyroidism: a pilot study. *Eur J Nucl Med Mol Imaging.* 2014;41:2083–2089.
12. Kubinyi J, Chroustova D, Fialovà M, et al. The role of PET/CT with 18Ffluorocholine in hyperparathyroidism: preliminary results in 15 patients. *Eur J Nucl Med Mol Imaging.* 2014:S284(abstract OP568).
13. Michaud L, Burgess A, Huchet V, et al. Is 18Ffluorocholine-PET/CT a new imaging tool for detecting hyperfunctioning parathyroid glands in primary or secondary hyperparathyroidism? *J Clin Endocrinol Metab.* 2014;2014:2014;99:4531–4536.
14. Johnson NA, Carty SE, Tublin ME. Parathyroid imaging. *Radiol Clin N Am.* 2011;49:489–509.
15. Haber RS, Kim CK, Inabnet WB. Ultrasonography for preoperative localization of enlarged parathyroid glands in primary hyperparathyroidism: comparison with (^{99m})technetium sestaMIBI scintigraphy. *Clin Endocrinol.* 2002;57:241–249.
16. Périé S, Fessi H, Tassart M, et al. Usefulness of combination of high resolution ultrasonography and dual phase dual-isotope iodine ^{123}/technetium Tc^{99m} sestaMIBI scintigraphy for the preoperative localization of hyperplastic parathyroid glands in renal hyperparathyroidism. *Am J Kidney Dis.* 2005;45:344–352.

17. Wakamatsu H, Noguchi S, Yamashita H, et al. Parathyroid scintigraphy with ^{99m}Tc-MIBI and ^{123}I subtraction: a comparison with magnetic resonance imaging and ultrasonography. *Nucl Med Commun.* 2003;24:755–762.
18. Krausz Y, Lebensart PD, Klein M, et al. Preoperative localization of parathyroid adenoma in patients with concomitant thyroid nodular disease. *World J Surg.* 2000;24:1573–1578.
19. Barczynski M, Golkowski F, Konturek A, et al. Technetium-^{99m}-sestaMIBI subtraction scintigraphy vs. ultrasonography combined with a rapid parathyroid hormone assay in parathyroid aspirates in preoperative localization of parathyroid adenomas and in directing surgical approach. *Clin Endocrinol (Oxf).* 2006;65:106–113.
20. Sukan A, Reyhan M, Aydin M, et al. Preoperative evaluation of hyperparathyroidism: the role of dual-phase parathyroid scintigraphy and ultrasound imaging. *Ann Nucl Med.* 2008;22:123–131.
21. Lumachi F, Marzola MC, Zucchetta P, et al. Hyperfunctioning parathyroid tumours in patients with thyroid nodules. Sensitivity and positive predictive value of high-resolution ultrasonography and ^{99m}Tc-sestaMIBI scintigraphy. *Endocr Relat Cancer.* 2003;10:419–423.
22. Awad SS, Miskulin J, Thompson N. Parathyroid adenomas versus four-gland hyperplasia as the cause of primary hyperparathyroidism in patients with prolonged lithium therapy. *World J Surg.* 2003;27:486–488.
23. Marti JL, Yang CS, Carling T, et al. Surgical approach and outcomes in patients with lithium-associated hyperparathyroidism. *Ann Surg Oncol.* 2012;19:3465–3471.
24. Tunninen V, Varjo P, Schildt J, et al. Comparison of five parathyroid scintigraphic protocols. *Int J Mol Imaging.* 2013:921260. doi: 10.1155/2013/921260.
25. Schalin-Jantti C, Ryhänen E, Heiskanen I, et al. Planar scintigraphy with ^{123}I/^{99m}Tc-sestaMIBI, ^{99m}Tc-sestaMIBI SPECT/CT, 11C-methionine PET/CT, or selective venous sampling before reoperation of primary hyperparathyroidism. *J Nucl Med.* 2013;54:739–747.
26. Hassler S, Ben-Sellem D, Hubele F, et al. Dual-isotope ^{99m}Tc-MIBI/^{123}I parathyroid scintigraphy in primary hyperparathyroidism: comparison of subtraction SPECT/CT and pinhole planar scan. *Clin Nucl Med.* 2014;39:32–36.
27. Gul K, Ozdemir D, Korukluoglu B, et al. Preoperative and postoperative evaluation of thyroid disease in patients undergoing surgical treatment of primary hyperparathyroidism. *Endocr Pract.* 2010;16:7–13.
28. Arciero CA, Shiue ZS, Gates JD, et al. Preoperative thyroid ultrasound is indicated in patients undergoing parathyroidectomy for primary hyperparathyroidism. *J Cancer.* 2012;3:1–6.
29. Eccles A, Challapalli A, Khan S, et al. Thyroid lymphoma incidentally detected by 18F-fluorocholine (FCH) PET/CT. *Clin Nucl Med.* 2013;38:755–757.
30. Karps JS, Surti S, Daube-Witherspoon ME, et al. The benefit of time-of-flight in PET imaging experimental and clinical. *J Nucl Med.* 2008;49:462–470.
31. Sisson JC, Thompson NW, Ackerman RJ, et al. Use of 2- [F-18]-fluoro-2-deoxy-D-glucose PET to locate parathyroid adenomas in primary hyperparathyroidism. *Radiology.* 1994;192:280.
32. Melon P, Luxen A, Hamoir E, et al. Fluorine-18-fluorodeoxyglucose positron emission tomography for preoperative parathyroid imaging in primary hyperparathyroidism. *Eur J Nucl Med.* 1995;22:556–558.
33. Neumann DR, Esselstyn CB, Maclntyre WJ, et al. Comparison of FDG-PET and sestaMIBI-SPECT in primary hyperparathyroidism. *J Nucl Med.* 1996;37:1809–1815.
34. Chicklore S, Schulte KM, Talat N, et al. 18F-FDG PET rarely provides additional information to 11C-methionine PET imaging in hyperparathyroidism. *Clin Nucl Med.* 2014;39:237–242.
35. Caldarella C, Treglia G, Isgro MA, et al. Diagnostic performance of positron emission tomography using 11C-methionine in patients with suspected parathyroid adenoma: a meta-analysis. *Endocrine.* 2013;43:78–83.
36. Lange-Nolde A, Zajic T, Slawik M, et al. PET with 18FDOPA in the imaging of parathyroid adenoma in patients with primary hyperparathyroidism: a pilot study. *Nuklearmedizin.* 2006;45:193–196.
37. Balogova S, Talbot JN, Nataf V, et al. 18Ffluorodihydroxyphenylalanine vs other radiopharmaceuticals for imaging neuroendocrine tumours according to their type. *Eur J Nucl Med Mol Imaging.* 2013;40:943–966.
38. Tunninen V, Kauppinen T, Eskola H, et al. Parathyroid scintigraphy protocols in Finland in 2010. Results of the query and current status. *Nuklearmedizin.* 2010;49:187–194.
39. Greenspan BS, Dillehay G, Intenzo C, et al. SNM practice guideline for parathyroid scintigraphy 4.0. *J Nucl Med Technol.* 2012;40:111–118.
40. Nakagami K, Uchida T, Ohwada S, et al. Increased choline kinase activity and elevated phosphocholine levels in human colon cancer. *Jpn J Cancer Res.* 1999;90:419–424.
41. Melloul M, Paz A, Koren R, et al. ^{99m}Tc-MIBI scintigraphy of parathyroid adenomas and its relation to tumour size and oxyphil cell abundance. *Eur J Nucl Med.* 2001;28:209–213.
42. Westreich RW, Brandwein M, Mechanick JI, et al. Preoperative parathyroid localization: correlating false-negative technetium ^{99m} sestaMIBI scans with parathyroid disease. *Laryngoscope.* 2003;113:567–572.